ORIGIN OF ALBITE PODS IN THE GEORDIE LAKE GABBRO, PORT COLDWELL ALKALINE COMPLEX, NORTHWESTERN ONTARIO: EVIDENCE FOR LATE-STAGE HYDROTHERMAL Cu–Pd MINERALIZATION

DAVID J. GOOD AND JAMES H. CROCKET

Department of Geology, McMaster University, Hamilton, Ontario L8S 4M1

ABSTRACT

Disseminated sulfides and palladium minerals are spatially associated with albite pods in the Geordie Lake (GL) gabbro, located in the north-central part of the Port Coldwell alkaline complex, northwestern Ontario. The pods range from less than a centimeter to meters across and consist predominantly of albite (Ab_{95-99}) and minor amounts of hornblende, biotite and actinolite. The hornblende contains up to 2.5 wt.% F and crystallized prior to biotite and actinolite. The pods are typically surrounded by a zone, less than about 20 cm thick, of very coarse-grained GL gabbro. In these zones, olivine is strongly zoned, plagioclase is rimmed by albite–oligoclase, and the relative proportion of the minerals varies significantly. The abundances of Zr, Hf, Nb, Th, U and *REE* in the albite pods are high relative to GL gabbro, and interelement ratios for the two rock types are equivalent. The data indicate that albite pods represent pockets of fluid-enriched residual magma. The albite probably formed by a two-stage process. In step one, hornblende and plagioclase crystallized from the residual magma. In step two, a hydrous fluid separated from the residual magma and interacted with the plagioclase to form albite. This model is consistent with textural evidence, the high F content of hornblende, and the fractionation trends exhibited by the alkalis in the albite pods. Comparison with experimental data indicates that the albite formed at a temperature below about 600°C. The sulfides consist of chalcopyrite and bornite, and minor amounts of sphalerite, pyrite and galena. They are invariably intergrown with biotite ± actinolite and were deposited after the formation of albite. The close spatial association of biotite, actinolite, sulfides, palladium minerals and albite implies that they formed from a single fluid, but at different times as the temperature decreased and the composition of the fluid evolved. The fluid probably was derived from the highly evolved magma that formed the albite pods.

Keywords: platinum-group elements, albite, zoned olivine, autointrusion, late-stage hydrothermal sulfide, Geordie Lake gabbro, Port Coldwell alkaline complex, Ontario.

SOMMAIRE

Les sulfures et les minéraux de palladium disséminés dans le gabbro du lac Geordie, situé dans le secteur nord-central du complexe alcalin de Port Coldwell, dans le nord-ouest de l'Ontario, montrent une association étroite avec des amas d'albite. Ceux-ci vont de moins d'un centimètre jusqu'à une échelle métrique, et contiennent surtout de l'albite (Ab_{95-99}) et une proportion moins importante de hornblende, biotite et actinote. La hornblende contient jusqu'à 2.5% de fluor (en poids), et a cristallisé avant la biotite et l'actinote. Les amas d'albite sont typiquement entourés d'une zone de moins de 20 cm de gabbro à grains très grossiers. Dans ces zones, l'olivine est très fortement zonée, le plagioclase montre un liseré d'albite ou d'oligoclase, et la proportion des minéraux varie de façon marquée. La concentration de Zr, Hf, Nb, Th, U, et des terres rares dans les amas d'albite est élevée par rapport au gabbro; par contre, les rapports entre éléments sont les mêmes dans les deux types de roches. Nos données montrent que les amas d'albite représenteraient des poches de magma résiduel enrichi en phase fluide. Nous croyons que l'albite s'est formée en deux stades. D'abord, hornblende et plagioclase ont cristallisé à partir du magma résiduel. Ensuite, la phase fluide, séparée du magma résiduel, a transformé le plagioclase en albite. Ce modèle concorde avec l'évidence texturale, la teneur élevée en fluor de la hornblende, et le tracé de fractionnement dont font preuve les alcalins dans les amas d'albite. Une comparaison avec les données expérimentales montre que l'albite se serait formée à une température inférieure à 600°C. Les sulfures, chalcopyrite et bornite, avec sphalérite, pyrite et galène accessoires, sont intimement associés à biotite ± actinote, et sont apparus une fois l'albite formée. La relation étroite parmi biotite, actinote, sulfures, minéraux de palladium et albite fait penser qu'ils se sont formés à partir de la même phase fluide, mais à divers stades de son évolution et de son refroidissement. Cette phase fluide serait issue du magma responsable des amas d'albite.

(Traduit par la Rédaction)

Mots-clés: éléments du groupe du platine, albite, olivine zonée, sulfures hydrothermaux tardifs, gabbro de Geordie Lake, complexe alcalin de Port Coldwell, Ontario.

INTRODUCTION

The association of chalcopyrite and platinum-group minerals (PGM) with secondary silicate minerals such as albite, biotite and actinolite in orthomagmatic settings is seen to be evidence for the transport and concentration of platinum-group elements by fluids (Rowell & Edgar 1986, Nyman *et al.* 1990, Mogessie

et al. 1991, Farrow & Watkinson 1992, Watkinson & Melling 1992, Watkinson & Ohnenstetter 1992). In each case, the fluids are presumed to be derived from either residual magma or country rock, and the PGE are remobilized from pre-existing magmatic sulfides at low to intermediate temperatures. In the Geordie Lake (GL) gabbro, located well within the Port Coldwell alkaline complex near Marathon, Ontario (Fig. 1),
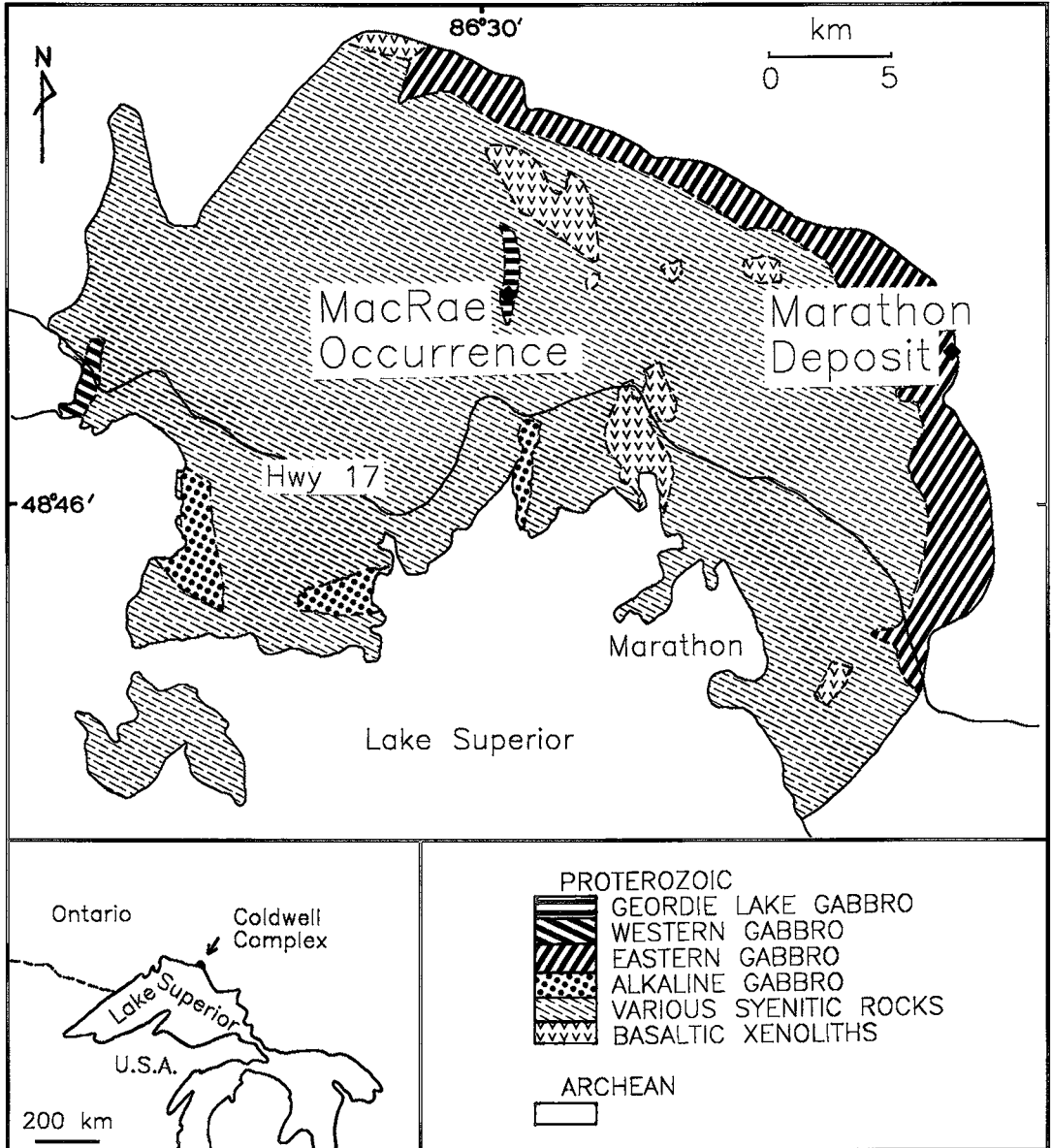

FIG. 1. Location of the MacRae occurrence and Marathon deposit in the Port Coldwell alkaline complex (modified after Walker *et al.* 1992). Previous detailed mapping of the syenitic rocks, including various nepheline-, quartz- and amphibole-bearing syenites, is omitted to highlight the location of gabbroic rocks.
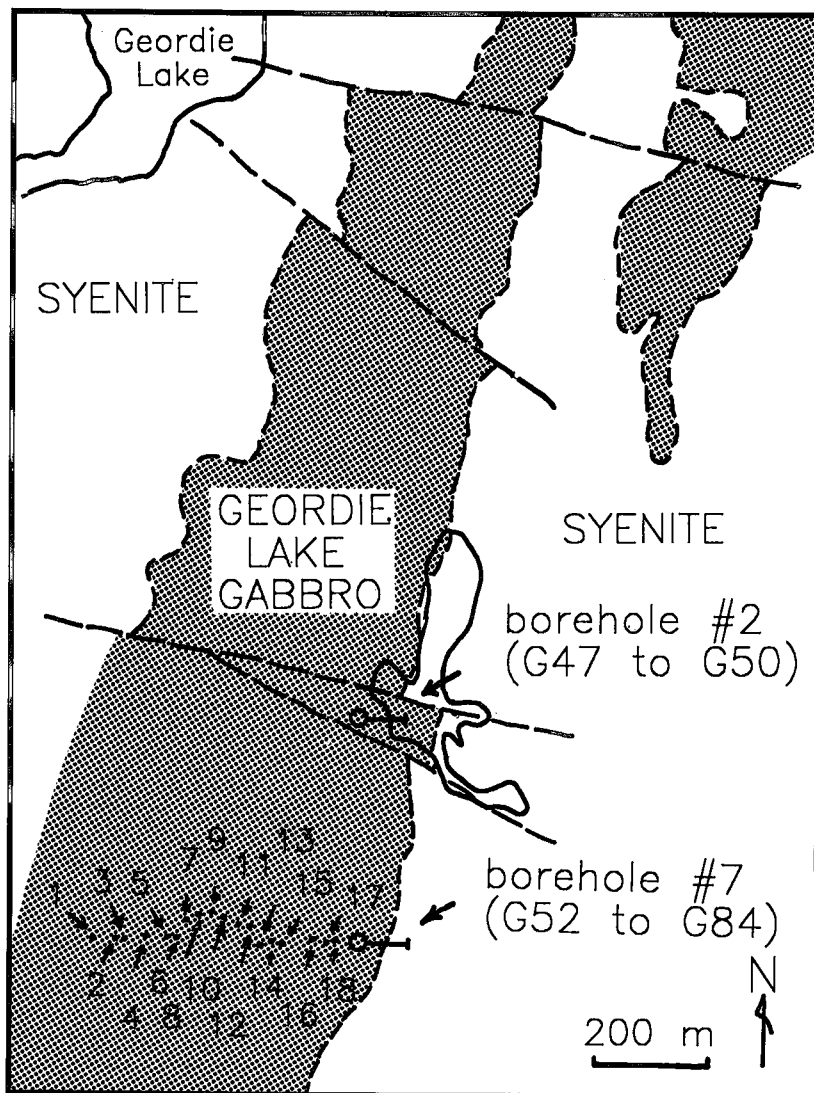
FIG. 2. Geological map of a portion of the Geordie Lake gabbro (after St. Joe Canada Inc., now Bond Gold, 1987) indicating sample locations. All samples are referred to with a G prefix in the text. The geology of syenitic rocks is poorly defined.

palladium minerals are associated with chalcopyrite that is intergrown with biotite, actinolite and albite. In mineralized samples, abundances of Cu and Pd are as high as 1.1 wt.% and 800 ppb, respectively, but Ir is not concentrated above background values (Good 1993). Although these features imply a fluid control for the formation of sulfides and PGM, several characteristics of the host gabbro imply that this deposit formed by a process that is different than those relating to other deposits of hydrothermal origin. For instance, a prominent feature of this deposit is the close spatial association of PGM and sulfides with albite pods that are surrounded by a zone, less than

about 20 cm thick, of very coarse-grained gabbro. Previously, the pods were interpreted to be zones of intense hydrothermal alteration where primary gabbroic minerals were replaced by albite and actinolite (Mulja 1989, Mulja & Mitchell 1990), but Good & Crocket (1990) proposed that they represent accumulations of residual GL magma. Geochemical data gathered in this study support the latter hypothesis. By determining the origin of the albite pods and describing their relationships to the sulfides, it will be shown that highly evolved residual GL magma was a probable source for the mineralizing fluids, Cu and PGE.

GEOLOGY OF THE GEORDIE LAKE GABBRO

The Geordie Lake (GL) gabbro is located in the north-central part of the Port Coldwell alkaline complex (PCAC). The geological map of the PCAC (Fig. 1) is modified after Walker *et al.* (1992) to highlight the location of gabbroic rocks and the Marathon deposit (Watkinson & Ohnenstetter 1992, Good & Crocket 1994). The PCAC is a large composite intrusive body (Puskas 1967, Currie 1980, Mitchell & Platt 1982, Sage 1991, Walker *et al.* 1991, 1992, 1993) that was emplaced at 1108 ± 1 Ma (Heaman & Machado 1992) into Archean rocks of the Schreiber – White River granite–greenstone belt. It is associated with the Midcontinent Rift System, active between 1109 (Davis & Sutcliffe 1985) and 1086 Ma (Palmer & Davis 1987). The PCAC is situated off the axis of the rift system and considered to be related to other intrusive complexes of the Midcontinent Rift, such as the Duluth Complex and the Logan Sills (Mitchell & Platt 1978, Sutcliffe 1991, Heaman & Machado 1992).

The GL gabbro, a north–south-trending body approximately 500 by 4000 m in size, is bounded by poorly defined syenitic intrusions (Fig. 2). At the contact, the gabbro is medium grained, and the syenite is fine grained (<0.5 mm). Two meters from the contact, the syenite is medium to coarse grained. The chilled margin relationship implies that syenitic magma cut the gabbro. This order of emplacement is contrary to the previous interpretation of Mulja & Mitchell (1990). They proposed that GL gabbro cut the syenitic rocks, on the basis of recrystallization-induced textures in the syenite, and the distribution of sulfides. However, we interpret the granular nature of individual alkali feldspar grains in syenite near the contact to be braided perthite and not recrystallization-induced. Further, the distribution of sulfides cannot be considered as evidence to support the order of intrusion, as the migration of sulfides out of the gabbro and into the syenite could occur in either case.

Layering in the GL gabbro has not, as yet, been recognized in the field or by petrographic or geochemical methods; thus strike and dip of the intrusive body are not positively determined. Nevertheless, the main zone of disseminated sulfides and the contact between eastern gabbro and syenitic rocks trend nearly north and dip moderately west; consequently, samples were selected from east–west traverses (Fig. 2). In their examination of several suites of samples collected along east–west traverses, Mulja (1989) and Good (1993) found no evidence that would suggest east–west layering; consequently, our set of samples should be representative of the GL gabbro.

The GL gabbro is subdivided into homogeneous and heterogeneous types. This distinction is warranted because only the latter contains abundant sulfide and Pd mineralization. At the south end of the main unit of GL gabbro, heterogeneous gabbro occurs in a zone less than 100 m thick, located along the eastern contact with syenitic rocks. The two boreholes sampled in this study consist predominantly of heterogeneous gabbro. West of each borehole is abundant outcrop that forms a nearly complete section of homogeneous gabbro. At the north end of the main unit, outcrop is less abundant, and as a result, the spatial relationship between the gabbro types is poorly understood.

PETROLOGY AND MINERAL CHEMISTRY

Analytical methods

Compositions of clinopyroxene, plagioclase, and olivine were determined for samples from homogeneous and heterogeneous gabbro (Tables 1, 2 and 3, respectively). Compositions of biotite and amphibole were determined for mineralized samples only (Table 4). These were determined with the JEOL JXA–8600 Superprobe electron microprobe at the University of Western Ontario. Minerals were analyzed by comparison with several mineral standards.

TABLE 1. COMPOSITION OF CLINOPYROXENE IN THE GEORDIE LAKE GABBRO AND ALBITE POD

Sample no.	G2	G49	G50
Notes	1	2	3
SiO₂ wt.%	51.07	50.46	50.81
TiO₂	0.73	0.77	0.87
Al₂O₃	1.86	1.91	2.33
FeO	12.03	12.10	11.93
MnO	0.36	0.27	0.29
MgO	12.16	12.24	12.39
CaO	21.31	21.59	21.49
Na₂O	0.37	0.41	0.39
Total	99.89	99.75	100.5

Calculated on the basis of 6 atoms of oxygen

Si	1.941	1.926	1.920
^{IV}Al	0.059	0.074	0.025
^{VI}Al	0.024	0.012	0.080
Ti	0.021	0.022	0.024
Fe	0.382	0.386	0.377
Mn	0.012	0.009	0.009
Mg	0.689	0.697	0.698
Ca	0.868	0.883	0.870
Na	0.027	0.030	0.029
Fs	19.7	19.7	19.4
Wo	44.7	44.9	44.7
En	35.6	35.4	35.9

Location of samples: 1) in homogeneous gabbro (Fig. 3), 2) within albite pod, and 3) at m.–g. gabbro – pod contact (Fig. 8).

The electron beam was operated at 10.3 nA and 5 kV. The spot size was approximately 1 μm. Peak counting times were between 20 and 100 seconds, depending on the element. Levels of Ni in olivine were determined using 100-second counts and natural olivine as a standard (P140, see Fleet & MacRae 1983). Control of quality of the data was maintained by periodic analysis of standards during each session.

Homogeneous Geordie Lake gabbro

Homogeneous GL gabbro is medium to coarse grained and consists of subhedral to euhedral plagioclase, euhedral apatite, subhedral or skeletal magnetite, and anhedral to subhedral clinopyroxene. Homogeneity of the gabbro is exhibited by the relatively constant abundance of CIPW normative minerals in a section from the south-central part of the unit (Fig. 3). The abundance of normative minerals is used because a) secondary minerals have partly obscured original minerals, and b) they approximately match the estimated mode. Approximately 20 to 50% of each clinopyroxene crystal was altered to actinolite, but this may vary from about 5 to 90%. The edges of plagioclase crystals were modified to a cloudy albite to oligoclase. The modified plagioclase occurs within a ghost outline of the initial plagioclase. The modified plagioclase is cut by abundant microfractures that contain very fine-grained biotite and actinolite, and trace amounts of chalcopyrite and sphalerite. Biotite and actinolite also occur together in small interstitial patches. Magnetite is commonly rimmed by a thin zone of biotite.
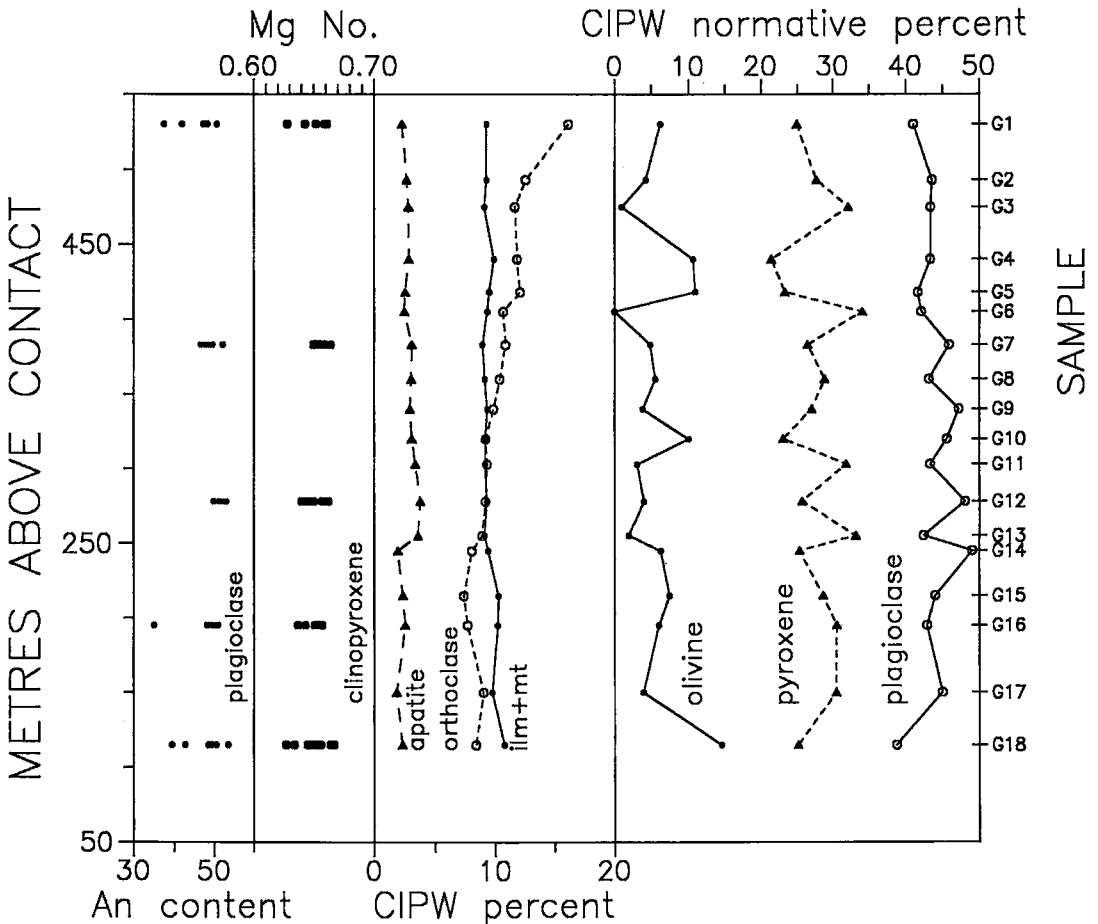

FIG. 3. CIPW normative abundances of minerals and compositions of plagioclase and clinopyroxene in a section of homogeneous Geordie Lake gabbro.

Plagioclase crystals are 5 to 10 mm in length and have high aspect-ratios (5–10). They are commonly oriented to form an east–west-trending lineation that plunges moderately west. Imbrication of plagioclase occurs locally (Fig. 4). Apatite is ubiquitous and occurs in two distinct textural habits consistent with two periods of growth. The most abundant and presumably earliest crystals are euhedral, 0.1 to 0.5 mm in cross section, and are typically included in magnetite and clinopyroxene. The second type of apatite is approximately one-tenth the size of the first and is enclosed within the albite to oligoclase rim.

There is no apparent variation in mineral compositions across the homogeneous gabbro (Fig. 3). The average compositions of plagioclase, excluding modified rims, and Mg/(Mg+Fe) values of clinopyroxene for five samples are An_{47} to An_{52} and 0.65 to 0.66, respectively (Fig. 3). Subhedral plagioclase is normally zoned, with core-to-rim variations of about 5% An. Discontinuous zonation, excluding modified rims, is rare.

Heterogeneous Geordie Lake gabbro

Heterogeneous GL gabbro exhibits compositional and textural variations on the centimeter scale (Fig. 5). In general, the variations are associated with albite pods. Heterogeneous gabbro consists of various proportions of plagioclase, clinopyroxene, olivine and magnetite. The average grain-size varies from about 1 mm to 2 cm. Olivine gabbro, gabbro, mela-olivine gabbro and troctolite are representative rock types. In general, the sequence of crystallization of primary minerals in all rock types is plagioclase, followed by magnetite, apatite and olivine, then clinopyroxene. This order is similar to that for homogeneous gabbro. Plagioclase is subhedral, and clinopyroxene is interstitial and anhedral. Olivine is typically subhedral to anhedral, but locally forms a harrisitic texture. Inter-

stitial, subhedral or skeletal magnetite and euhedral apatite are ubiquitous. Compositional heterogeneity across borehole 7 is shown by the variation of abundances of normative minerals (Fig. 6). These abundances do not agree, on the whole, with approximate modes because several samples contain very small pods of albite, and heterogeneity may occur on the centimeter scale, so that whole-rock compositions represent averages.

The compositions of plagioclase and clinopyroxene in the heterogeneous gabbro are very similar to those in the homogeneous gabbro. For heterogeneous gabbro, the composition of subhedral plagioclase varies between An_{45} and An_{57}, and the Mg/(Mg+Fe) value of clinopyroxene, between 0.40 and 0.67 (Mulja 1989). Also, like the section of homogeneous gabbro, there is an absence of significant or systematic variations in the composition of plagioclase and clinopyroxene (Mulja 1989).

Albite rims and pods

Abundant albite occurs throughout the heterogeneous gabbro as a rim on initial plagioclase and in irregular discontinuous pods (Fig. 5). The rims consist of albite to oligoclase (An_7 to An_{22}), hereafter referred to as "albite", and are visibly distinguished from subhedral plagioclase in thin section by their cloudiness; in hand sample, the rim is pink, and subhedral plagioclase is white. The albite pods are easily distinguished from gabbro by the light pink color and saccharoidal form of the albite grains. They range from less than a centimeter to a meter across. In general, the abundance of the rims increases approaching a pod, and the abundance of very small pods increases approaching a large pod.

The rims are typically 25 to 50% as thick as the subhedral plagioclase. They contain abundant micrometric inclusions of apatite, actinolite and K-feldspar
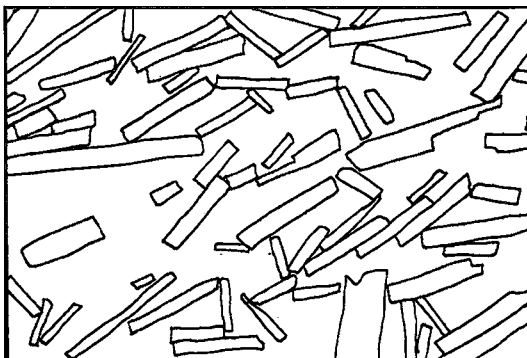

FIG. 4. Drawing of imbrication texture for plagioclase crystals in homogeneous gabbro. The width of the field of view is 3 cm.

FIG. 5. Characteristics of albite pods and heterogeneous GL gabbro. A. Irregular, discontinuous albite pod (light grey). B. Close-up view of the tip of the albite pod, located left of center at the top of photo A, showing the granular albite and interstitial biotite and actinolite in the pod and the gradational coarse-grained contact with gabbro. C and D. Photographs of oversized thin sections indicate coarse-grained plagioclase, clinopyroxene and magnetite around very small albite pods (C) (see also Fig. 9) and at the contact of larger albite pods (D), respectively. The opaque phases consist predominantly of magnetite and minor chalcopyrite intergrown with actinolite and biotite. The cloudy rims on plagioclase are albite–oligoclase.
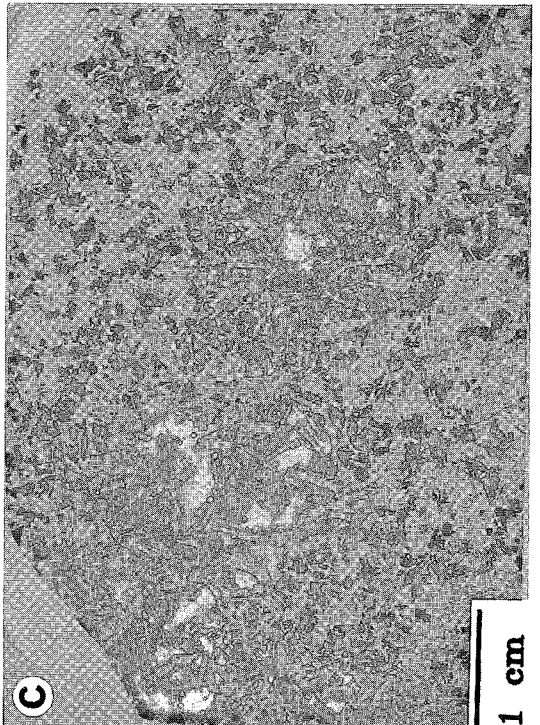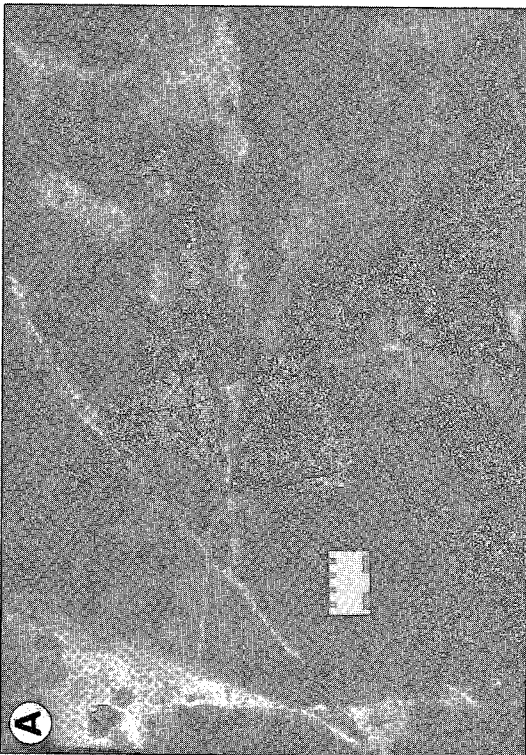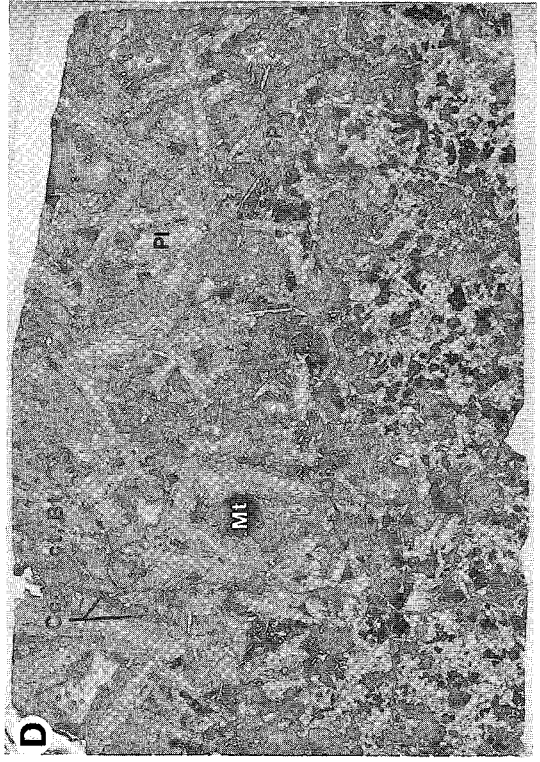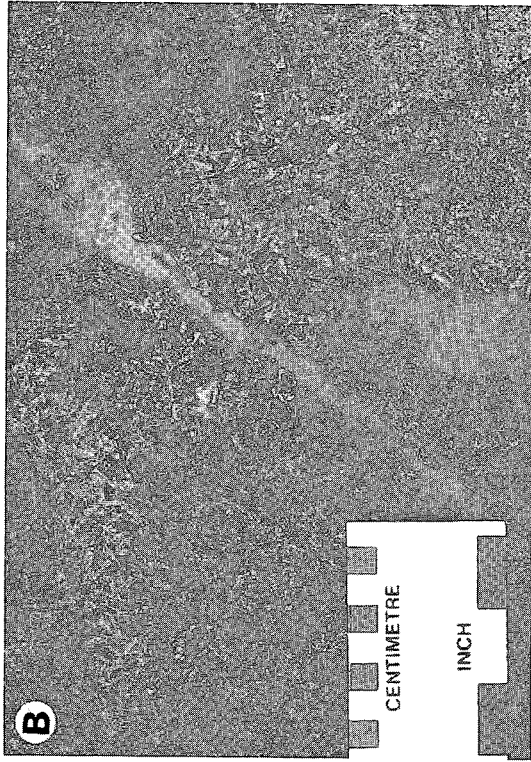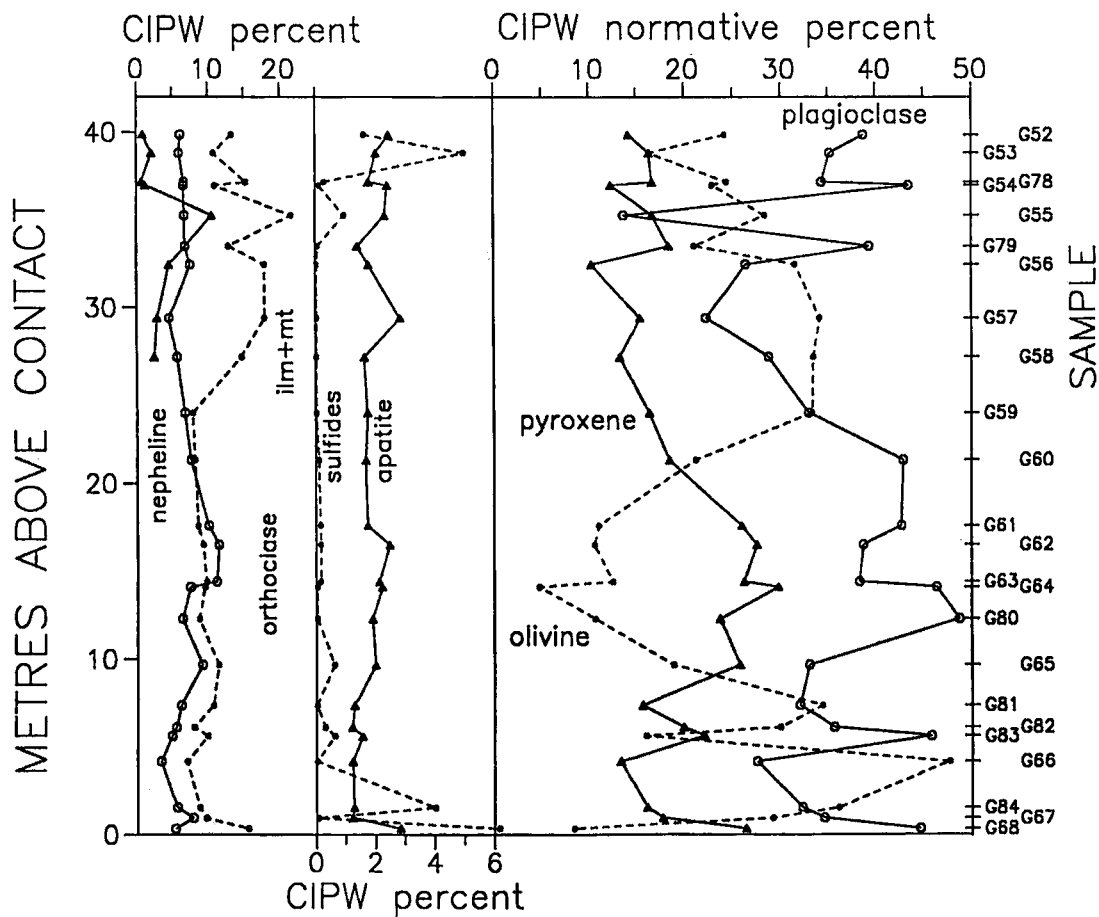
FIG. 6. CIPW normative abundances of minerals across a section of heterogeneous GL gabbro.

(Fig. 7) and minor amounts of Ba–K-feldspar (Table 2). The contact between a rim and the initial plagioclase is gradational from straight and abrupt to diffuse and irregular. The abrupt change in compositions across a straight contact is illustrated by two microprobe analyses separated by a distance of approximately 15 μm, located near point A in Figure 7. Here, the composition of the primary plagioclase is $An_{48}Or_{0.46}$; the rim is $An_{15}Or_{0.17}$. Also, at sharp contacts, neighboring clinopyroxene is partly replaced (Fig. 7). At diffuse, irregular contacts, a ghost outline of the initial subhedral plagioclase is observable in the albite rim. The variation of compositions across a diffuse contact is shown by decreasing An and Or contents over approximately 100 μm near point B in Figure 8B. These features imply that two processes acted to produce the rims: replacement and modification of initial minerals. The straight sharp contacts imply that a rim formed around the initial crystals of

plagioclase, and that the mineral(s) that originally surrounded the plagioclase were replaced. The diffuse irregular contacts imply that the initial plagioclase was partly modified to a more sodic composition. In general, where replacement is predominant, the nearby clinopyroxene and olivine are only slightly altered to actinolite; where plagioclase modification is predominant, such as in homogeneous gabbro, they are more intensely altered.

Albite pods consist of albite, hornblende, biotite, sulfides and actinolite, and trace amounts of K-feldspar, quartz, zircon, allanite, apatite, and calcite. The albite is granular or lath-like, fine- to medium-grained, and cloudy. Hornblende makes up approximately 1% of albite pods, and is pale brown, fine-grained and subhedral to anhedral. Biotite and actinolite are very fine grained and occur together either in small patches interstitial to albite and hornblende, or in microfractures that cut albite. Allanite
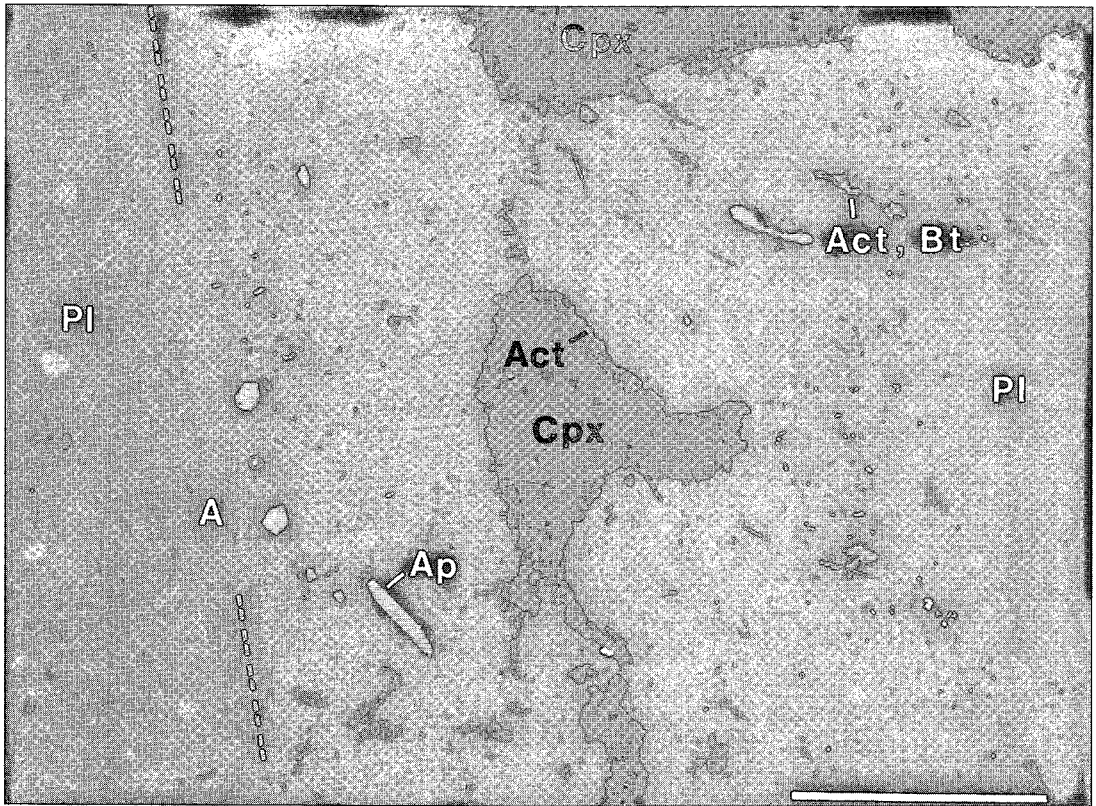
FIG. 7. Back-scattered electron image of albite–oligoclase rim on plagioclase (black) and replacement of clinopyroxene. Near point A, the contact between rim (An_{15}) and plagioclase (An_{48}) is sharp (see text). The rims are separated by the partly replaced clinopyroxene in the center of the photo. Each rim is optically continuous and is distinguished from early plagioclase by the inclusions of apatite (white) and intergrowths of biotite and actinolite (light grey). The clinopyroxene crystals [Mg/(Mg+Fe) value of 0.64] have a very thin margin of actinolite and are optically continuous with an ophitic crystal to the right of the photo. Scale bar: 100 μm.

crystals are included within biotite, calcite and chalcopyrite. Calcite occurs as a late mineral that replaces actinolite, or in patches approximately 100 μm in size, that contain many euhedral crystals of zircon 1 to 5 μm across.

The large pods commonly include minerals from the GL gabbro. The compositions and habits of included clinopyroxene and plagioclase are identical to those in the surrounding gabbro. The included plagioclase is partly modified to a more sodic composition; clinopyroxene crystals are irregular and have a very

TABLE 2. FELDSPAR COMPOSITIONS REPRESENTATIVE OF DISTINCT TEXTURAL AND PETROGRAPHIC SETTINGS IN GEORDIE LAKE GABBRO

Sample Notes	G47 1	G47 2	G58 3	G58 4	G52 5	G52 6	G50 7	G49 8
SiO_2	55.20	56.63	65.26	65.97	56.55	65.78	69.22	69.50
Al_2O_3	27.55	26.60	23.54	18.82	21.44	21.56	19.40	19.31
FeO	0.59	0.52	0.05	0.00	0.08	0.27	0.02	0.04
Na_2O	5.07	5.58	7.97	1.29	0.19	9.69	9.65	9.89
K_2O	0.31	0.59	0.14	14.24	11.86	0.04	0.03	0.03
CaO	10.53	9.23	4.49	0.10	0.36	2.62	0.49	0.33
BaO	0.01	0.08	0.00	0.48	11.24	0.54	0.00	0.00
Total	99.26	99.23	101.45	100.90	101.72	100.50	98.81	99.10
	structural formulae calculated on the basis of 32 atoms of oxygen							
Si	10.036	10.271	11.300	12.005	11.060	11.543	12.127	12.144
Al	5.905	5.688	4.803	4.036	4.941	4.459	4.006	3.978
Fe	0.090	0.079	0.007	0.000	0.013	0.039	0.002	0.006
Na	1.787	1.962	2.676	0.455	0.072	3.296	3.279	3.351
K	0.072	0.137	0.031	3.305	2.959	0.009	0.007	0.007
Ca	2.051	1.794	0.833	0.019	0.075	0.493	0.092	0.062
Ba	0.001	0.006	0.000	0.034	0.861	0.037	0.000	0.000
Ab	45.70	50.40	75.59	12.04	1.80	86.79	97.07	97.98
Or	1.84	3.52	0.87	87.44	74.59	0.23	0.21	0.20
An	52.46	46.08	23.53	0.52	1.90	12.98	2.72	1.81
Celsian					21.70			

Notes: 1 and 2, core and rim of subhedral plagioclase lath, respectively; 3, modified plagioclase located in Fig. 9d; 4, anhedral potassium feldspar (Ksp) located in modified plagioclase rim in Fig. 9d; 5, barian potassium feldspar located in modified plagioclase rim; 6, oligoclase rim on plagioclase in Fig. 7; 7, average of 3 analyses from 3 grains in very small albite pod (Fig. 8); 8, average of 9 analyses from 6 grains in albite pod.
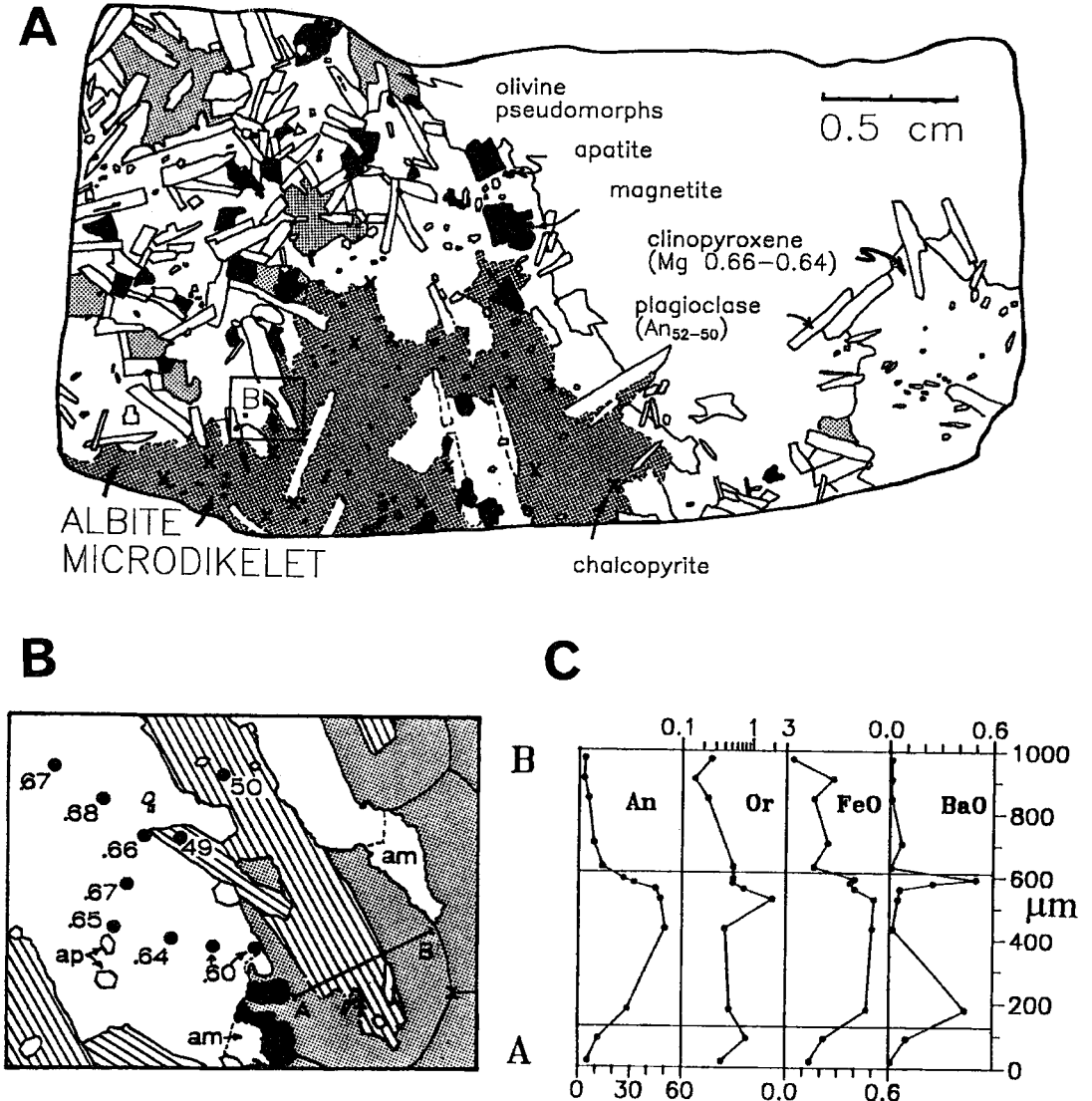
FIG. 8. Relationships at a sharp contact, between gabbro and a small albite pod (microdikelet), from sample G50. A. Drawing of a thin section of gabbro that includes a small albite pod (shaded). Sulfides (X) consist of chalcopyrite ± shalerite, are intergrown with biotite ± actinolite, and are located within the albite pod. Olivine is completely altered to actinolite plus magnetite. B. Close-up drawing of minerals at the contact (location outlined in A) showing optically continuous grains of albite and the Mg/(Mg+Fe) value of clinopyroxene (white). Clinopyroxene has a very thin rim of actinolite where it is in contact with albite. C. Compositional cross-section of plagioclase from points A to B in Fig. 8B.

thin fringe of actinolite; olivine is altered to an actinolite plus magnetite pseudomorph, and magnetite grains are embayed and rimmed by biotite and actinolite. Apatite in small pods exhibits a well-defined bimodal distribution of grain size. The large grains are approximately 0.5 mm in cross section, and the small grains are less than 0.1 mm (compare apatite in Fig. 9C to

that in Figs. 7, 9D).

The texture and composition of the GL gabbro adjacent to the albite pods were examined; there are two possible relationships. In the first type, the texture, grain size and compositions of clinopyroxene and plagioclase are identical to that of gabbro elsewhere (*e.g.*, Fig. 8). In the second type, the microdikelets and pods

FIG. 9. Relationships at a gradational contact between gabbro and small albite pod, from sample G58. A and B. Photograph and drawing, respectively, of a thin section with coarse-grained gabbro around an albite pod. Olivine grains 1, 2 and 3 are strongly zoned (Table 3). The composition of plagioclase (grain 4) is identical to that in medium-grained gabbro. C. Photomicrograph of the box outlined in B showing the modification of plagioclase during the formation of albite. D. Back-scattered electron image of the box outlined in C showing inclusions of apatite (Ap), K-feldspar (Kf) and actinolite (Act) in modified plagioclase. Numbers (24 and 48) refer to anorthite content of plagioclase (Table 2).
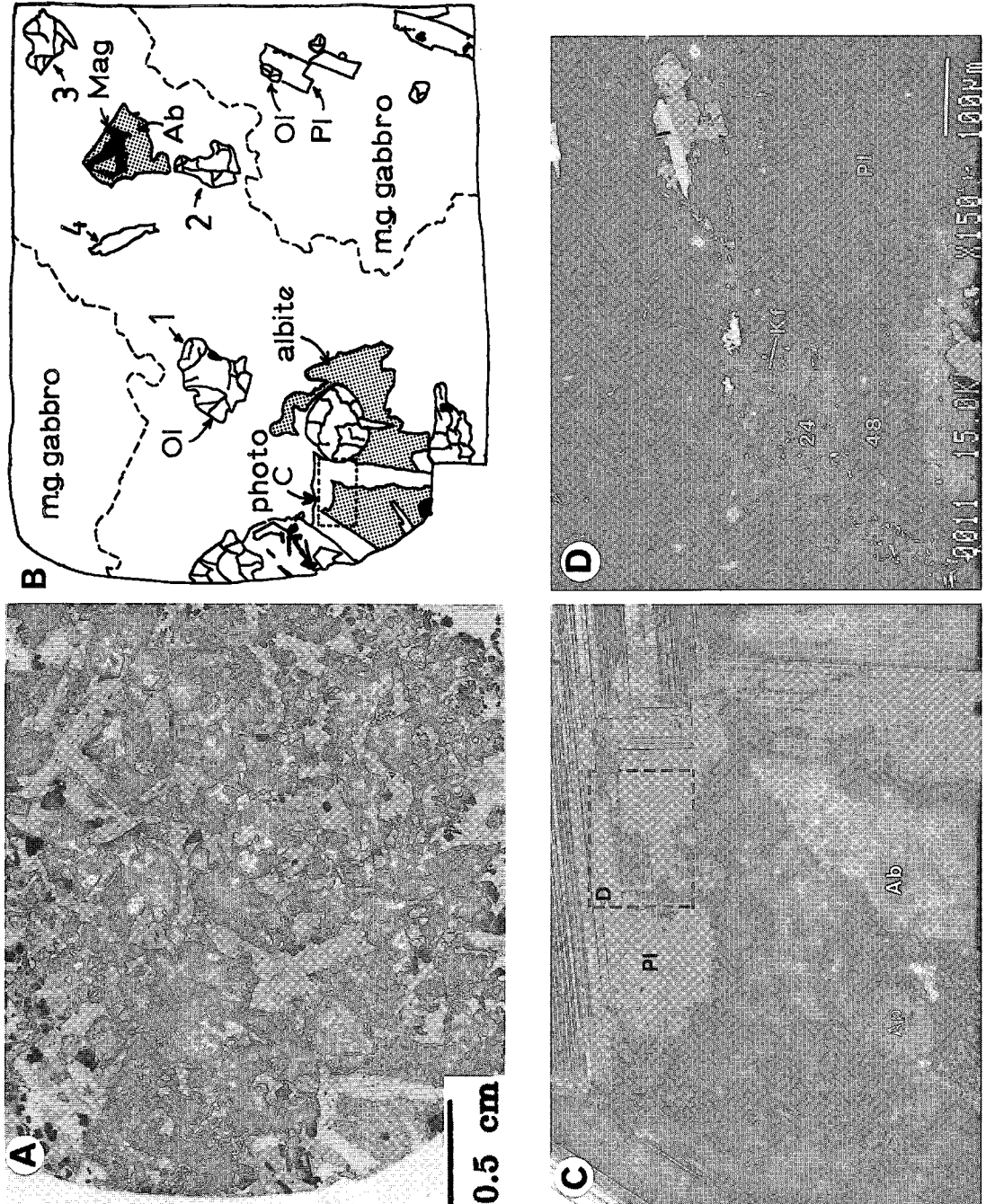
are surrounded by a very coarse-grained zone of gabbro with variable proportions of the major minerals (Figs. 5, 9). Here, plagioclase laths are up to 2 cm long; clinopyroxene grains are up to 1 cm, and olivine and magnetite are up to 0.5 cm. Three olivine grains in a coarse-grained zone were analyzed (grains 1, 2 and 3 in Fig. 9A, B, Table 3); they are all zoned. Core and rim compositions on grains 2 and 3 are Fo_{49} and Fo_{40}, respectively, and Fo_{35} and Fo_{29} on grain 1. The Ni contents vary from less than detection limit (300 ppm) to 500 ppm. These zoned crystals of olivine are very unusual, as the mineral is known to re-equilibrate easily during crystallization, and consequently is rarely zoned. Indeed, Mulja (1989) found that olivine in GL gabbro is unzoned. Two subhedral grains of plagioclase from this zone were analyzed (grain 4 in Figs. 9B, D); they are identical in composition to plagioclase in the medium-grained gabbro.

Sulfides and platinum-group minerals

Sulfides consist predominantly of chalcopyrite and bornite, with minor amounts of sphalerite, pyrite and galena. The sulfide grains are typically less than 0.1 mm across and occur as isolated grains, or in clusters less than one cm across. At the scale of a thin section, sulfides occur only in the presence of albite (*e.g.*, Fig. 8). In general, the abundance of sulfides increases with the abundance of albite; however, in albite pods, the distribution of sulfides is irregular. The sulfides are invariably intergrown with biotite or actinolite. The sulfide + biotite ± actinolite assemblages are located, in decreasing order of occurrence, in a) microfractures that cut albite grains or the rim of albite to oligoclase on plagioclase, b) interstitially to partly altered minerals of the gabbro or albite grains, c) intergrown with actinolite after clinopyroxene, and d) along cleavage planes of magnetite or clinopyroxene. Locally, calcite replaces actinolite and surrounds chalcopyrite grains.

A complex association of ten palladium minerals, sperrylite, various tellurides, chalcopyrite and bornite are described in detail by Mulja & Mitchell (1990, 1991). They stated that most of the palladium minerals and tellurides are contained within the disseminated chalcopyrite (described above). The Pd minerals include kotulskite, merenskyite, michenerite, sopcheite, paolovite, guanglinite, palladium bismutholtelluride, arsenide and antimonide, and unnamed $Pd_{1.6}NiAs_{1.5}$; the tellurides include hessite, unnamed Ag_3Te_2, melonite and altaite (Mulja & Mitchell 1991).

Abundance of fluorine and chlorine in hydrous minerals

The relative abundances of fluorine and chlorine in hornblende, biotite and actinolite (Table 4) are shown in Figure 10. In general, hornblende contains 0.3 to

TABLE 3. COMPOSITIONS OF ZONED OLIVINE LOCATED IN COARSE–GRAINED GABBRO ADJACENT TO ALBITE POD

Grain no. location	2 core	2 interm	2 rim	1 core	1 rim
SiO2	34.79	34.45	33.58	32.82	32.09
TiO2	0.05	0.04	0.07	0.10	0.06
Al2O3	0.03	0.07	0.01	0.03	0.03
FeO	42.30	43.90	47.67	51.25	54.72
MnO	0.89	0.79	1.07	1.08	1.30
MgO	22.93	20.63	18.60	15.71	12.69
CaO	0.05	0.87	0.06	0.33	0.33
Ni	400	500	300	dl	300
Total	101.12	100.87	101.16	100.50	101.28

Structural formulae calculated on the basis of 4 atoms of oxygen

Si	0.993	0.989	0.988	0.984	0.984
Al	0.001	0.002	0.000	0.001	0.001
Ti	0.001	0.002	0.002	0.002	0.000
Fe	1.010	1.055	1.173	1.285	1.403
Mn	0.022	0.021	0.027	0.027	0.034
Mg	0.976	0.898	0.816	0.702	0.580
Ca	0.002	0.028	0.027	0.011	0.011
Ni	0.001	0.001	0.001	0.000	0.001
Fa	50.9	54.4	59.0	64.7	70.8
Fo	49.1	45.6	41.0	35.3	29.2

Note: dl represents value less than detection limit of 200 ppm Ni. Grains 1 and 2 are located less than 1 cm from a small pod of albite (G58, Fig. 9). Microprobe analyses were carried out at core, intermediate and rim locations. Results in wt.% except for Ni, in ppm.

2.5 wt.% F and less than 0.1% Cl; biotite contains approximately 0.5% F and Cl, and actinolite contains 0.1 to 0.3% F and less than 0.2% Cl. The very high F/Cl ratio in hornblende relative to biotite and actinolite is consistent with petrographic evidence that hornblende crystallized from an evolved magma, and biotite and actinolite crystallized from a hydrous fluid.

GEOCHEMISTRY

Analytical methods

All whole-rock geochemical analyses were carried out at McMaster University. The major elements and Ba, V, Nb, Rb, Sr, Y and Zr were determined by X-ray fluorescence (XRF). The concentrations of the *REE*, Cl, Ta, Th, Hf, Cs and Sc were determined by instrumental neutron-activation analysis (INAA) on approximately 0.5 g of rock powder, except for Gd, which was determined by prompt gamma activation analysis. Uranium concentrations were determined by delayed
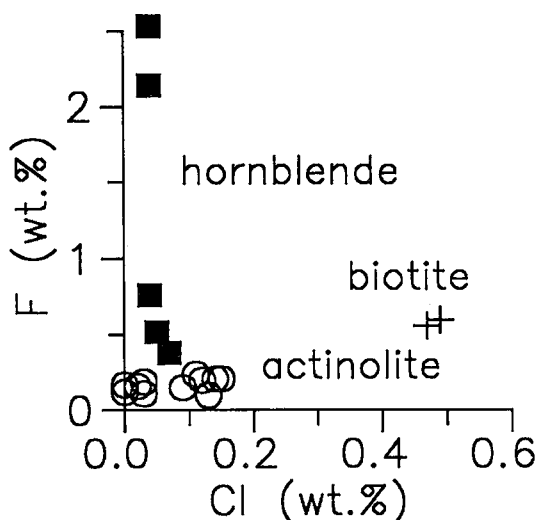
FIG. 10. Plot of F *versus* Cl in hornblende, biotite and actinolite associated with albite pods. Biotite is intergrown with chalcopyrite in microveinlets that cut albite. Actinolite occurs as a secondary rim on hornblende and clinopyroxene and is intergrown with biotite.

TABLE 4. COMPOSITIONS OF HORNBLENDE, ACTINOLITE, BIOTITE ASSOCIATED WITH ALBITE PODS

Mineral	Bt	Hbl	Hbl	Act	Act
Sample	G50	G49	G50	G50	G50
Notes	1	2	3	4	5
SiO_2 wt.%	36.62	43.31	42.73	50.53	53.71
TiO_2	2.26	2.26	2.33	0.27	0.12
Al_2O_3	13.38	7.83	8.47	4.14	1.91
MnO	0.13	0.28	0.31	0.51	0.52
FeO	23.10	17.51	17.32	17.94	16.72
MgO	10.98	10.25	10.47	11.77	12.75
CaO	0.22	10.95	11.09	11.67	12.14
BaO	0.28	–	–	–	–
K_2O	8.05	1.43	1.51	0.26	0.09
Na_2O	0.09	2.69	2.17	0.85	0.41
F	0.59	2.53	0.52	0.24	0.19
Cl	0.48	0.04	0.05	0.11	0.03
Total	96.19	99.09	96.97	98.29	98.59
–O=F,Cl	0.36	1.07	0.23	0.13	0.09
Total	95.83	98.02	96.74	98.16	98.50

Structural formulae calculated on the basis of 24 O,OH,F,Cl

Si	5.633	6.497	6.547	7.463	7.809
Al	2.367	1.384	1.453	0.537	0.191
Al	0.059	0.000	0.077	0.183	0.136
Ti	0.261	0.255	0.268	0.030	0.013
Mn	0.017	0.036	0.040	0.064	0.064
Fe	2.972	2.197	2.219	2.216	2.033
Mg	2.518	2.292	2.391	2.591	2.763
Ca	0.036	1.760	1.821	1.847	1.891
Ba	0.017				
K	1.579	0.274	0.295	0.049	0.017
Na	0.027	0.782	0.645	0.243	0.116
F	0.287	1.200	0.252	0.112	0.087
Cl	0.125	0.010	0.013	0.028	0.007
Mg/(Mg+Fe)	0.46	0.51	0.52	0.54	0.58

Notes: 1, biotite intergrown with chalcopyrite within microvein that cuts albite in pod; 2, hornblende in albite pod; 3, hornblende in contact with clinopyroxene within albite pod; 4, thin actinolite rim on hornblende of previous column (4); 5, thin actinolite rim on clinopyroxene.

neutron counting. The effects of primary interference reactions produced by U fission on the abundances of Sm, La, Nd and Ce, as reported by Landsberger (1986) and Landsberger & Simsons (1987), were evaluated and found to be negligible. The accuracy of XRF data is within 4% for all elements. The precision (standard error of the mean of four determinations) of INAA data is better than 6% for all elements, except Ho (12%), Th (10%) and Cs (18%).

Results

Major- and trace-element concentrations for a suite of samples representative of the GL gabbro and albite pods are presented in Table 5. The principal goal of the geochemical study is to constrain a possible genesis for the albite pods. The problem is approached by first evaluating the variations in trace-element concentrations across a section of homogeneous gabbro in order to distinguish possible trends due to processes such as crystal fractionation or metasomatism. Once the trends are established, they are compared to trace-element concentrations in the heterogeneous gabbro and albite pod.

A modified cross-section of homogeneous gabbro is presented in Figure 11. Data for a representative suite of samples are presented in Table 6. In order to smooth out the curves and make the trends more prominent, data are modified in three steps. Firstly, each value is divided by the respective concentration in sample G47 in order to simplify the horizontal

scale. Sample G47 was selected to normalize the values because it has a minimum of secondary minerals, such as an albite rim on plagioclase and actinolite alteration of clinopyroxene, and because plagioclase and clinopyroxene compositions are equivalent to those in the sample set. In the second step, the data are converted into three-point moving-average values, *i.e.*, each point is the average of itself plus two neighboring values. Finally, step two is repeated to further smooth out the trends.

The modified elemental trends in Figure 11 are grouped according to slope, as follows: 1) U, Nb, Zr, Rb, K, and Cu: concentrations increase significantly

up-section from sample G18 to G2, 2) Ba and Y: concentrations increase slightly up-section, 3) Sr: the concentration is approximately constant through much of the section, but decreases near the top, and 4) Ni and V: concentrations decrease up-section.

The trend for Cu is erratic, but the increase up-section implies classification into group one. The increase in chlorine concentrations is much larger than for group 1, but is not assigned its own class for reasons discussed below. These data, except those for Cl, resemble those of a fractionating silicate magma whereby clinopyroxene, plagioclase, magnetite and possibly apatite are the dominant crystallizing phases. Thus, elements in group 1 are highly incompatible; group-2 elements are moderately incompatible, group-3 elements are weakly compatible, and group-4 elements are compatible.

The trace-element concentrations for homogeneous gabbro are compared to those of heterogeneous gabbro on element *versus* Zr variation diagrams (Fig. 12). Samples of heterogeneous gabbro are subdivided into

TABLE 6. ABUNDANCES OF TRACE AND MINOR ELEMENTS ACROSS THE HOMOGENEOUS GABBRO

		G18	G16	G12	G7	G2	% [1]
K$_2$O	wt%	1.38	1.27	1.52	1.79	2.08	51
P$_2$O$_5$		0.96	1.06	1.57	1.27	1.11	16
Ni	ppm	46	33	21	17	16	−65
V		673	547	523	382	343	−49
Y		43	34	48	42	50	16
Rb		52	41	56	69	94	81
Nb		36	39	46	50	70	94
Zr		171	176	210	221	285	67
U		2.46	2.60	2.91	3.13	4.00	63
Cl		522	829	1501	1202	2927	460

%[1]: Percent change corresponds to change from samples G18 to G2. Refer to sample locations on Figure 2 and modified geochemical trends in Figure 11.

three groups: gabbro with rare to minor albite rims on plagioclase, gabbro with small albite pods, and albite pod. In general, the diagrams, except for Rb and Cl, indicate that data for the heterogeneous gabbro are colinear and partly overlap those for homogeneous gabbro. The highly incompatible elements, Hf, Nb, U, Th and Zr, are enriched in the albite pod relative to homogeneous gabbro; compatible elements Sc and V are depleted.

Concentrations of the rare-earth elements in various types of gabbro and albite pods are compared on a chondrite-normalized diagram (Fig. 13). The nearly parallel trends and the ascending order of sample concentrations are consistent with trends exhibited in Figures 12C to H. The approximate 2- to 3-fold increase in the abundance of *REE* from sample G47 to albite pod (G49) is about one half of the 6- to 7-fold increase shown by the highly incompatible elements, implying that the *REE* behaved as moderately incompatible elements during formation of the albite pods. This relationship is consistent with the moderately incompatible behavior of Y in homogeneous gabbro (Fig. 11). The moderately incompatible behavior of Y and *REE*, and the nearly parallel trends for Y and P in Figure 11, indicate control by crystallization of small amounts of apatite. Partition coefficients between apatite and melt are on the order of 10 to 50 (Fujimaki 1986), depending on the element; consequently, crystallization of 1% apatite corresponds to a bulk partition-coefficient of 0.1 to 0.5.

The coincident behavior exhibited by trace elements in the homogeneous and heterogeneous gabbros does not apply to the alkalis and chlorine. For Rb and K$_2$O *versus* Zr (Figs. 12A, B), the data for heterogeneous gabbro are scattered relative to the nearly linear trend exhibited by homogeneous gabbro. Relative to gabbro, the albite pod has the highest concentration of Zr, but very low concentrations of Rb and Cl (Table 5). The behavior of alkalis (K, Rb, and

TABLE 5. GEOCHEMISTRY OF SAMPLES REPRESENTATIVE OF GEORDIE LAKE GABBRO AND ALBITE POD

Sample	G1	G2	G47	G48	G49	G49a	G50
Rock type	1	1	2	3	4	3	3
SiO2 wt%	48.46	48.17	40.57	42.23	52.05	45.85	45.36
Al2O3	13.11	13.40	11.21	12.95	15.42	13.22	13.12
Fe2O3	18.95	17.04	24.62	21.60	12.32	19.52	18.97
MgO	2.43	3.18	7.35	6.12	2.92	4.18	4.62
CaO	7.39	8.84	9.14	8.95	7.63	8.88	9.42
Na2O	3.10	3.08	1.75	2.01	5.35	3.01	2.81
K2O	2.68	2.08	1.42	1.97	0.85	0.93	1.26
TiO2	2.06	2.06	2.45	2.01	1.91	2.05	2.13
P2O5	0.95	1.11	0.94	0.90	0.73	1.27	1.50
MnO	0.31	0.26	0.30	0.26	0.21	0.24	0.25
Total	99.43	99.38	97.75	99.00	99.39	99.14	99.44
Rb ppm	140	94	37	62	13	35	44
Sr	394	555	462	611	433	673	659
Ba	1439	1330	697	1108	337	881	970
Y	52	50	20	28	60	43	36
Zr	312	285	86	104	564	198	153
V	242	343	792	615	259	515	476
Nb	84	70	19	28	117	59	34
Ta	6.27	5.41	2.07	2.36	8.46	4.14	3.22
U	4.45	4.00	0.98	1.54	6.89	2.73	2.33
Cl	5138	2927	1588	1422	644	676	995
Sc	23	26	29	25	17	22	25
Th	14.4	12.7	3.53	5.03	27	8.39	7.70
Hf	6.89	6.13	1.94	2.71	11	4.10	3.82
Cs	4.84	4.33	2.17	2.69	0.69	2.13	2.99
La	115	136	60	66	188	95	94
Ce	243	255	117	132	354	78	182
Nd	94	99	52	57	107	69	79
Sm	16.7	17.4	9.52	9.90	20	14	13.4
Eu	4.30	3.95	2.47	2.66	3.53	3.18	3.36
Gd	11.7	nd	6.39	7.42	14.1	9.67	10.2
Tb	1.47	1.53	0.64	0.89	1.58	1.16	0.99
Ho	1.84	1.75	0.79	0.92	2.10	1.65	1.25
Yb	4.08	3.89	1.76	1.91	5.04	3.16	2.29
Lu	0.69	0.66	0.30	0.32	0.69	0.53	0.43

Note: nd indicates not determined. Samples G47 to G50 were collected from a 1–m section of drill core in the order listed. Rock types as follows: 1, homogeneous gabbro; 2, olivine gabbro with no visible small pods of albite; 3, olivine gabbro with minor small pods of albite; 4, albite pod that includes fragments of GL gabbro.
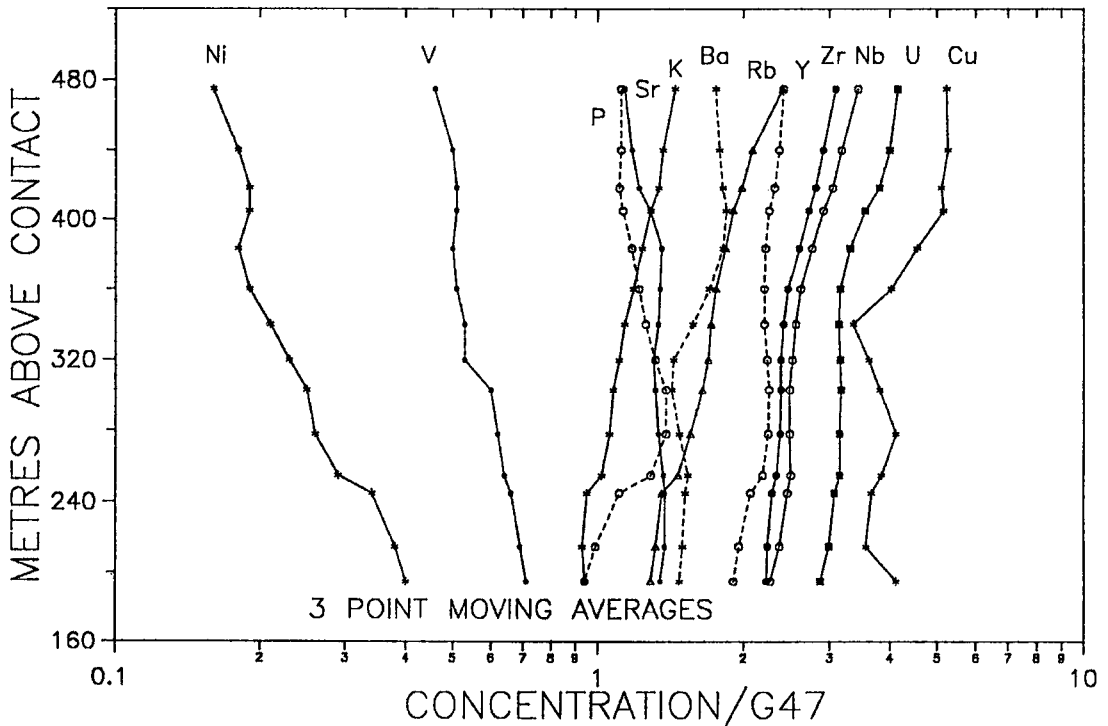
FIG. 11. Modified geochemical cross-section of homogeneous GL gabbro, based on samples G18 to G1 located in Fig. 2. Data are first normalized (divided) by the abundance of elements in sample G47. Each point is a three-point moving average (calculated twice) in order to make trends more prominent.

Cs) is further examined in Figure 14. The data for all GL gabbro samples, excluding the albite pods, fall within the main-trend envelope for igneous rocks as defined by Shaw (1968), and the K/Rb ratio varies between about 150 and 300. A smaller set of samples shown in Figures 14B and C indicates that Rb/Cs and K/Cs in GL gabbro, excluding the albite pod, are close to 20 and 5000, respectively. Therefore, it appears that K, Rb and Cs in the GL gabbro, excluding the albite pods, are behaving coherently. Three samples of albite pod are shown in Figure 14A. The solid star is from this study, and the two hollow stars are from Mulja (1989). The levels of K, Rb and Cs are depleted in the albite pods relative to the gabbro. The K/Rb and K/Cs ratios for the albite pods are greater than those for gabbro, and the Rb/Cs value in gabbro is equivalent to that in the albite pods. These relationships imply that Rb and Cs are fractionated from K. The whole-rock data are consistent with observed compositions of plagioclase from various settings within the homogeneous and heterogeneous gabbros, plotted in terms of Ab–Or–An (Fig. 15). These compositions form a continuum from labradorite to albite. This trend implies loss of K relative to Na. Thus during formation of the albite pods, the alkalis exhibit fractionation in the order Na – K – Rb = Cs.

DISCUSSION

Genesis of the homogeneous GL gabbro

The textures, field relations and mineral compositions observed in the homogeneous gabbro imply that it was emplaced as a plagioclase-crystal mush. Evidence for this process includes the imbrication of plagioclase (Fig. 4) and the uniform abundances and chemistry of major minerals (Fig. 3). Imbrication can only be interpreted to indicate flow of the magma and crystals. After intrusion, it seems unlikely that the crystal mush solidified *in situ*, as this process cannot explain the decoupling of trace-element from major-element data (Figs. 3, 11). Three possible mechanisms to account for the trends in Figure 11 are: 1) variable amounts of interstitial magma, 2) subsolidus metasomatism, and 3) migration of interstitial melt through the crystal pile. The first option is unlikely because it cannot account for the divergent trends of the *REE* relative to other incompatible trace elements. Also, higher proportions of interstitial melt should coincide with more evolved compositions of clinopyroxene, but this is not the case. Metasomatism might account for some observations, such as the ubiquitous partial alteration of clinopyroxene and plagioclase and the very
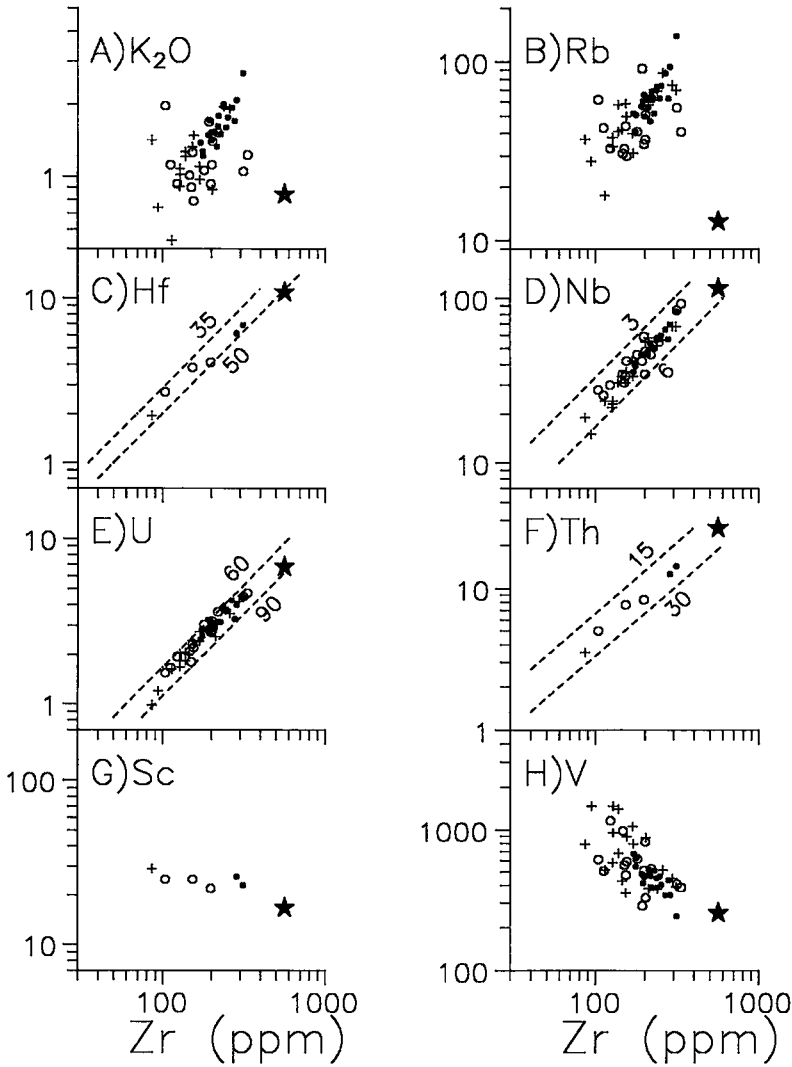
FIG. 12. Log–log plots of concentration of Zr *versus* that of various trace elements for GL gabbro. Symbols: homogeneous gabbro (dots), heterogeneous gabbro (+), heterogeneous gabbro with small albite pods (circles), albite pods (stars).

large increase in Cl concentrations, but trends for large-ion lithophile elements (K and Rb), which are typically mobile in hydrothermal fluids, closely match those for the relatively immobile, high-ionic-potential elements (U, Nb and Zr). Consequently, metasomatism alone cannot explain the data. The third possibility, the migration of interstitial melt through the pile of crystals, is the favored explanation. This process can account for the decoupling of major-element from trace-element data, and the subdivision of trace-element data into groups that are consistent with fractional crystallization of plagioclase, clinopyroxene,

magnetite and apatite. Possible mechanisms to explain migration of interstitial melt in the GL gabbro are compaction or composition convection, as described by Sparks *et al.* (1985). After intrusion, the GL crystal mush began crystallizing magnetite and clinopyroxene. Depending on the proportions of minerals crystallizing, the interstitial melt could become less dense than the pile of crystals and begin to move up through the pile. It is likely that migration occurred quite late in the crystallization history and involved a small fraction of the magma. This would account for the uniformity of clinopyroxene compositions.
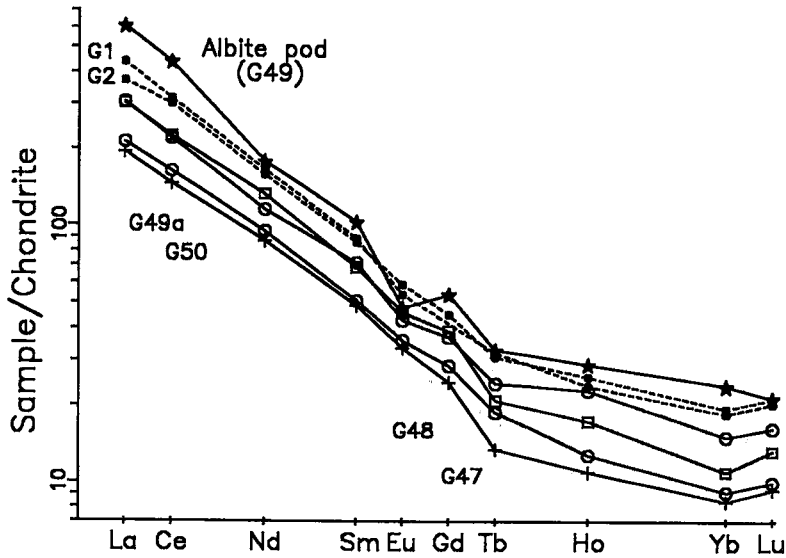
FIG. 13. Chondrite-normalized *REE* data for various rock types of GL gabbro. Symbols as in Fig. 12. Data are normalized using values in column 1 of Table 1.5 in Henderson (1984).

Eventually, as porosity became too low, migration of interstitial melt ended. In the later stages of crystallization, perhaps coincident with melt migration, a vapor exsolved from the highly evolved magma. Interaction of the vapor with gabbro resulted in the modification of labradorite to albite or oligoclase, formation of biotite, and the alteration of clinopyroxene to actinolite. Except for the excessive enrichment of Cl relative to the other trace elements, the deuteric alteration was essentially isochemical.

Origin of the albite pods by autointrusion

Geochemical characteristics of albite pods, such as very high concentrations of incompatible trace elements relative to GL gabbro and interelement ratios equivalent to those in GL gabbro, imply that they represent accumulations of highly evolved residual GL
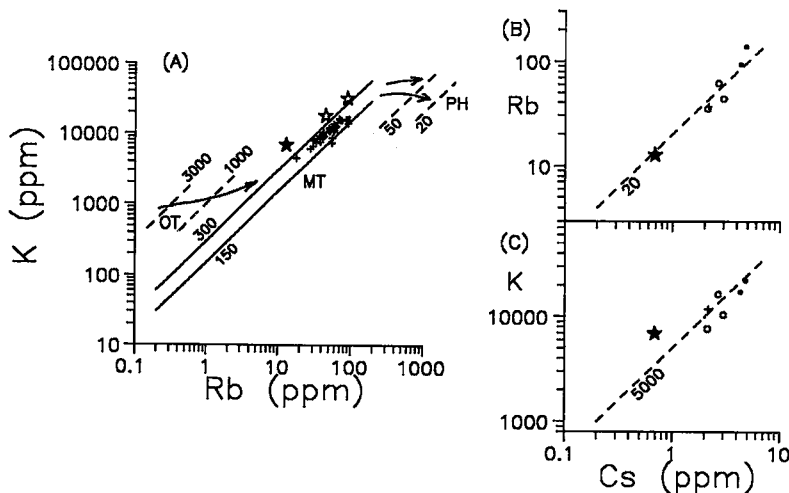

FIG. 14. Alkali variation diagrams for various rock types of GL gabbro. Symbols as in Fig. 12, except hollow stars from Mulja (1989).
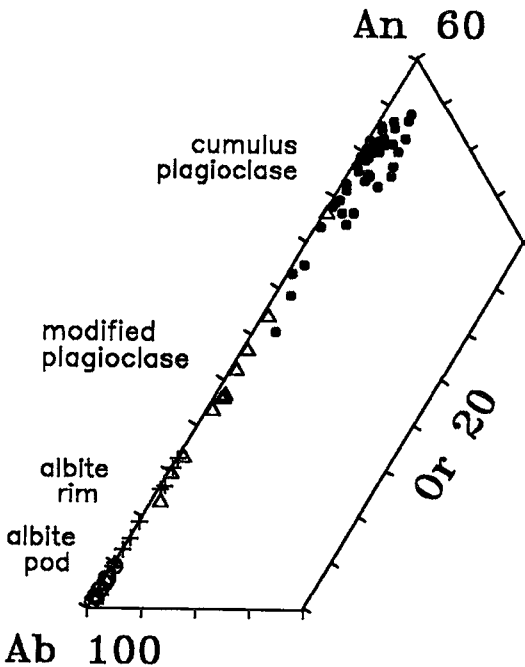
An 60

FIG. 15. Summary of plagioclase compositions from various textural settings in GL gabbro. Symbols: cumulus plagioclase, dots; modified plagioclase, triangles; albite rim, cross; and albite pod, circle.

magma. Thus the albite pods could represent segregations of locally derived interstitial magma or bodies of residual magma that intruded the pile of crystals. Petrographic features such as a) the uniformity of plagioclase and clinopyroxene compositions in medium-grained gabbro approaching the contacts with the albite pods, b) the development of a harrisitic texture, c) the presence of zoned olivine, and d) the occurrence of zones of very coarse-grained gabbro adjacent to the albite pods are consistent with either local segregation or autointrusion. However, given the geochemical evidence from the homogeneous gabbro that implies large-scale migration of interstitial melt through the pile of crystals, it is conceivable that albite pods formed by autointrusion.

The albite could not have been a primary mineral in equilibrium with the residual magma. The continuous trend of plagioclase compositions from labradorite to albite (Fig. 15) cannot be explained in terms of magmatic processes. For this reason, a sodic plagioclase is proposed to have crystallized along with hornblende in the early stages of formation of the albite pods.

The residual magma was volatile-rich. Evidence of a high content of volatiles includes the high F content of hornblende in albite pods (up to 2.5 wt.%, Table 4). Consequently, during cooling and crystallization of

the residual magma, it is likely that a fluid evolved and interacted with nearby minerals. This fluid is proposed to have modified the initial plagioclase to form albite. Hornblende was unaffected. This process is consistent with the high K/Rb and K/Cs ratios of pods relative to GL gabbro. The observed order of alkali fractionation from plagioclase into the vapor is, in ascending order, $Na \ll K < Cs = Rb$. That is, Na favors the feldspar, and Cs and Rb, the vapor. This order of partitioning is predicted by comparison of the size of the cation to the site it occupies in albite (see Lagache 1983, p. 251). For Ca, the distribution coefficient between albite and an aqueous chloride solution is strongly affected by temperature and pressure (Lagache 1983). A compilation of experimental data presented by Lagache (1983) indicates that at high temperature, Ca favors albite over vapor, and it is not until temperatures are less than about 600°C (at less than 2 kbar) that Ca begins to favor the vapor. Thus according to this model, modification of plagioclase to albite could not have occurred at temperatures above about 600°C. The release of K, Ca, and Ba from primary plagioclase into the fluid presumably promoted the formation of K-feldspar, Ba–K-feldspar, biotite and actinolite.

Origin of the heterogeneous GL gabbro

It is conceivable that compositional and textural heterogeneity in the GL gabbro formed during auto-intrusion. This model requires that the precursor to heterogeneous gabbro was homogeneous plagioclase-crystal mush. This condition is satisfied by geochemical and mineral chemistry data that imply that homogeneous and heterogeneous gabbros are cogenetic and were intruded at similar stages in their magmatic evolution. The model is as follows. At some point in the solidification history of the crystal mush, crystallization was interrupted by the intrusion of the highly evolved, volatile-rich residual magma that eventually formed the albite pods. Interaction between the two melts had numerous consequences. For instance, the forms and compositions of minerals growing in the crystal mush were modified by temperature differences between the two magmas and by migration of volatiles from the residual magma into the GL crystal mush. Undercooling resulted in the formation of the harrisitic texture and zoned olivine. The addition of volatiles facilitated the formation of very coarse-grained crystals. Also, the addition of volatiles changed the phase relations and resulted in variations in the relative proportions of minerals crystallizing in the mush.

The proposed genesis of the heterogeneous GL gabbro differs from that put forward by Mulja (1989) and Mulja & Mitchell (1991). They proposed that the GL gabbro formed by multiple intrusions of like magma, based on the alternating layers of troctolite

and ophitic gabbro, and the occurrence of the harrisitic texture. However, we were unable to distinguish any layers of troctolite. Indeed, in numerous samples identified as troctolite by Mulja (1989), the abundance of normative minerals is consistent with that of gabbro. This discrepancy cannot be due to alteration, but is possibly due to an overestimation of the modal abundance of the harrisitic texture in the heterogeneous gabbro. Also, we believe that the presence of the harrisitic texture is evidence for the migration of interstitial melt (see Donaldson 1982), and is not a quench product formed when successive pulses of basaltic magma intruded the gabbro, as previously proposed.

Proposed mechanism for concentrating Cu and Pd

The genetic model for the formation of the albite pods can also be applied to the concentration of Cu and Pd. A three-stage model is required. In step one, interstitial magma that eventually formed the albite pods became progressively enriched in Cu and Pd as it migrated through the pile of crystals. In step two, the residual magma intruded and interacted with the GL crystal mush to form heterogeneous gabbro. In step three, a hydrous fluid separated from the residual magma and extracted the ore-forming elements (Cu, Pd, S, As, Bi, Te, Sb). The vapor then reacted with plagioclase to form albite (T < 600°C) and migrated along grain boundaries into the surrounding gabbro. Precipitation of the sulfides and platinum-group minerals could occur in response to decreasing temperature, alteration of primary minerals or deposition of biotite and actinolite. This model differs from the magmatic sulfide origin proposed by Mulja & Mitchell (1990, 1991). The absence of pentlandite and pyrrhotite in the assemblage of sulfides, the scattered distribution of Ni, Cu and platinum-group elements (Good 1993), the temperature of mineralization (<600°C, this study; <550°C, Mulja & Mitchell 1991) and the association of chalcopyrite and Pd minerals with albite, biotite and actinolite are consistent with deposition from a hydrous fluid and cannot be explained by a magmatic sulfide model.

The concentration of PGE by postcumulus fluid-dominated processes was proposed by Watkinson & Ohnenstetter (1992) to have played an important role in the formation of the Marathon deposit, located 18 km east of the GL gabbro at the eastern margin of the complex (Fig. 1). However, a comparison of numerous petrographic and geochemical features of mineralization of the two deposits suggests that they formed by very different processes. Observations from the GL gabbro imply that metals and fluid were derived from highly evolved magma, and the sulfides and PGM were precipitated in association with biotite and actinolite. There is no evidence for pre-existing magmatic sulfides in the GL gabbro. At the Marathon deposit, geochemical observations described by Good

& Crocket (1994) imply that the petrographic and mineral chemistry data described by Watkinson & Ohnenstetter (1992) are best interpreted to represent a deuteric overprinting of primary magmatic sulfides. It is evident that the bulk sulfides were not enriched in Cu and the PGE by this process, as previously proposed, and that the migration of Cu and PGE in fluids occurred over very short distances.

CONCLUSIONS

The occurrence of chalcopyrite and palladium minerals in association with albite, biotite and actinolite in the Geordie Lake gabbro presumably represents the late-stage hydrothermal products of the solidification of the GL magma. The petrographic, mineral chemistry and geochemical data may be interpreted as follows.

The GL gabbro intruded as a plagioclase-crystal mush. At some point during *in situ* crystallization, the interstitial magma began to migrate through the pile of crystals. Small accumulations of residual melt intruded, and interacted with, partly crystallized GL gabbro, resulting in the formation of heterogeneous gabbro. Crystallization of the volatile-rich residual melt resulted in the formation of sodic plagioclase and hornblende. Eventually, a fluid separated from the residual melt, extracting Cl and the ore-forming elements. The fluid also reacted with the plagioclase to form albite. The release of K, Ca and Ba during modification of plagioclase resulted in the deposition of K-feldspar and Ba–K-feldspar from the fluid. After the albite had formed, biotite, actinolite, allanite, chalcopyrite, galena, sphalerite and palladium minerals were deposited from the fluid as it migrated along crystal boundaries and through small fractures that cut albite, magnetite and clinopyroxene.

REFERENCES

CURRIE, K.L. (1980): The alkaline rocks of Canada. *Geol. Surv. Can., Bull.* **239**.

DAVIS, D.W. & SUTCLIFFE, R.H. (1985): U–Pb ages from the Nipigon plate and northern Lake Superior. *Geol. Soc. Am., Bull.* **96**, 1572-1579.

DONALDSON, C.H. (1982): Origin of some of the Rhum harrisite by segregation of intercumulus liquid. *Mineral. Mag.* **45**, 201-209.

FARROW, C.E.G. & WATKINSON, D.H. (1992): Alteration and the role of fluids in Ni, Cu and platinum-group element deposition, Sudbury Igneous Complex contact, Onaping–Levack area, Ontario. *Mineral. Petrol.* **46**, 67-83.

FLEET, M.E. & MACRAE, N.D. (1983): Partition of Ni between olivine and sulfide and its application to Ni–Cu sulfide deposits. *Contrib. Mineral. Petrol.* **83**, 75-81.

FUJIMAKI, H. (1986): Partition coefficients of Hf, Zr, and REE between zircon, apatite, and liquid. *Contrib. Mineral. Petrol.* **94**, 42-45.

GOOD, D.J. (1993): *Genesis of Copper – Precious Metal Sulfide Deposits in the Port Coldwell Alkalic Complex, Ontario*. Ph.D. thesis, McMaster Univ., Hamilton, Ontario. *Ont. Geol. Surv., Open- File Rep.* **5839**.

———— & CROCKET, J.H. (1990): PGE study: the MacRae and Marathon copper – precious metal deposits, Coldwell complex. *In* Geoscience Research Grant Program, Summary of Research 1989-1990. *Ont. Geol. Surv., Misc. Pap.* **150**, 87-96.

———— & ———— (1994): Genesis of the Marathon Cu–PGE deposit, Port Coldwell Alkalic Complex, Ontario: a Midcontinent Rift related magmatic sulfide deposit. *Econ. Geol.* **89**, 131-149.

HEAMAN, L.M. & MACHADO, N. (1992): Timing and origin of midcontinent rift alkaline magmatism, North America: evidence from the Coldwell Complex. *Contrib. Mineral. Petrol.* **110**, 289-303.

HENDERSON, P. (1984): General geochemical properties and abundances of the rare earth elements. *In* Rare Earth Element Geochemistry. Elsevier, New York (1-32).

LAGACHE, M. (1983): The exchange equilibrium distribution of alkali and alkaline-earth elements between feldspars and hydrothermal solutions. *In* Feldspars and Feldspathoids – Structures, Properties and Occurrences (W.L. Brown, ed.). NATO Adv. Study Inst., D. Reidel Publ. Co., Boston (247-279).

LANDSBERGER, S. (1986): Spectral interferences from uranium fission in neutron activation analysis. *Chem. Geol.* **57**, 415-421.

———— & SIMSONS, A. (1987): Quantification of uranium, thorium and gadolinium spectral interferences in instrumental neutron activation analysis of samarium. *Chem. Geol.* **62**, 223-226.

MITCHELL, R.H. & PLATT, G.R. (1978): Mafic mineralogy of ferroaugite syenite from the Coldwell alkaline complex, Ontario, Canada. *J. Petrol.* **19**, 627-651.

———— & ———— (1982): Mineralogy and petrology of nepheline syenites from the Coldwell alkaline complex, Ontario, Canada. *J. Petrol.* **23**, 186-214.

MOGESSIE, A., STUMPFL, E.F. & WEIBLEN, P.W. (1991): The role of fluids in the formation of platinum-group minerals, Duluth Complex, Minnesota: mineralogic, textural and chemical evidence. *Econ. Geol.* **86**, 1506-1518.

MULJA, T. (1989): *Petrology, Geochemistry, and Platinum-Group Element Mineralization of the Geordie Lake Intrusion, Coldwell complex, Ontario*. M.Sc. thesis, Lakehead Univ., Thunder Bay, Ontario.

———— & MITCHELL, R.H. (1990): Platinum-group minerals and tellurides from the Geordie Lake intrusion, Coldwell complex, northwestern Ontario. *Can. Mineral.* **28**, 489-501.

———— & ———— (1991): The Geordie Lake intrusion, Coldwell complex, Ontario: a palladium- and tellurium-rich disseminated sulfide occurrence derived from an evolved tholeiitic magma. *Econ. Geol.* **86**, 1050-1069.

NYMAN, M.W., SHEETS, R.W. & BODNAR, R.J. (1990): Fluid-inclusion evidence for the physical and chemical conditions associated with intermediate-temperature PGE mineralization at the New Rambler deposit, southeastern Wyoming. *Can. Mineral.* **28**, 629-638.

PALMER, H.C. & DAVIS, D.W. (1987): Paleomagnetism and U–Pb geochronology of volcanic rocks from Michipicoten Island, Lake Superior, Canada: precise calibration of the Keweenawan polar wander track. *Precambrian Res.* **37**, 157-171.

PUSKAS, F.P. (1967): Port Coldwell area. *Ontario Department of Mines, Preliminary Map* **P.114**.

ROWELL, W.F. & EDGAR, A.D. (1986): Platinum-group element mineralization in a hydrothermal Cu–Ni sulfide occurrence, Rathbun Lake, northeastern Ontario. *Econ. Geol.* **81**, 1272-1277.

SAGE, R.P. (1991): Alkalic rock, carbonatite and kimberlite complexes of Ontario, Superior Province. *In* Geology of Ontario (P.C. Thurston, H.R. Williams, R.H. Sutcliffe & G.M. Stott, eds.). *Ont. Geol. Surv., Spec. Vol.* **4**, 683-709.

SHAW, D.M. (1968): A review of K–Rb fractionation trends by covariance analysis. *Geochim. Cosmochim. Acta* **32**, 573-601.

SPARKS, R.S.J., HUPPERT, H.E., KERR, R.C., MCKENZIE, D.P. & TAIT, S.R. (1985): Postcumulus processes in layered intrusions. *Geol. Mag.* **122**, 555-568.

SUTCLIFFE, R.H. (1991): Proterozoic geology of the Lake Superior area. *In* Geology of Ontario (P.C. Thurston, H.R. Williams, R.H. Sutcliffe & G.M. Stott, eds.). *Ont. Geol. Surv., Spec. Vol.* **4**, 627-660.

WALKER, E.C., SUTCLIFFE, R.H., SHAW, C.S.J., SHORE, G.T. & PENCZAK, R.S. (1991): Geology of the Coldwell alkaline complex. *In* Summary of Field Work and Other Activities 1991. *Ont. Geol. Surv., Misc. Pap.* **157**, 107-116.

———, ———, ———, ——— & ——— (1992): Geology of the Port Coldwell alkalic complex. *In* Summary of Field Work and Other Activities 1992, *Ont. Geol. Surv., Misc. Pap.* **160**, 108-119.

———, ———, ———, ——— & ——— (1993): Precambrian geology of the Coldwell alkalic complex. *Ontario Geol. Surv., Open-File Rep.* **5868**.

WATKINSON, D.H. & MELLING, D.R. (1992): Hydrothermal origin of platinum-group mineralization in low-temperature copper sulfide-rich assemblages, Salt Chuck Intrusion, Alaska. *Econ. Geol.* **87**, 175-184.

——— & OHNENSTETTER, D. (1992): Hydrothermal origin of platinum-group mineralization in the Two Duck Lake intrusion, Coldwell Complex, northwestern Ontario. *Can. Mineral.* **30**, 121-136.